Journal of Statistical Physics, Vol. 66, Nos. 5/6, 1992

Natural Boundaries for Area-Preserving Twist Maps

A. Berretti,[1] A. Celletti,[2] L. Chierchia,[1] and C. Falcolini[1]

Received August 27, 1991

We consider KAM invariant curves for generalizations of the standard map of the form $(x', y') = (x + y', y + \varepsilon f(x))$, where $f(x)$ is an odd trigonometric polynomial. We study numerically their analytic properties by a Padé approximant method applied to the function which conjugates the dynamics to a rotation $\theta \mapsto \theta + \omega$. In the complex ε plane, natural boundaries of different shapes are found. In the complex θ plane the analyticity region appears to be a strip bounded by a natural boundary, whose width tends linearly to 0 as ε tends to the critical value.

KEY WORDS: Conservative dynamical systems; KAM theory; natural boundaries; Padé approximants.

1. INTRODUCTION

The purpose of this paper is to continue and extend the analysis, started in refs. 1 and 2, of the complex analytic properties of invariant curves for area-preserving twist diffeomorphisms (for a review, see, e.g., refs. 3 and 4).

We consider the following class of area-preserving twist maps F_ε: $(x, y) \mapsto (x', y')$ of the cylinder $\mathscr{C} \equiv \mathbb{T} \times \mathbb{R}$ into itself:

$$y' = y + \varepsilon f(x) \tag{1}$$

$$x' = x + y' \pmod{2\pi} \tag{2}$$

where $f(x)$ is an odd trigonometric polynomial (therefore with vanishing mean value) and ε a real parameter. Such maps generalize the so-called "standard map," where $f(x) = \sin x$.

[1] Dipartimento di Matematica, II Università degli Studi di Roma (Tor Vergata), 00133 Rome, Italy.

[2] Dipartimento di Matematica Pura e Applicata, Università di L'Aquila, 67100 Coppito-L'Aquila, Italy.

0022-4715/92/0300-1613$06.50/0

Given a number ω such that $\omega/2\pi$ is Diophantine, namely

$$\exists \gamma, \tau \geqslant 1 \quad \text{such that} \quad \forall n \in \mathbb{Z}\setminus\{0\}, \quad m \in \mathbb{Z}: \quad \left|\frac{\omega}{2\pi} n + m\right| \geqslant \frac{1}{\gamma |n|^{\tau}} \tag{3}$$

KAM theory tells that, for $|\varepsilon|$ small enough, there exists an invariant curve $\Gamma = \Gamma_\omega(\varepsilon) \subset \mathscr{C}$, homotopically nontrivial (i.e., which winds around the cylinder), invariant under F_ε $[F_\varepsilon(\Gamma_\omega) = \Gamma_\omega]$ and with rotation number ω. By a theorem of Birkhoff, such curves are graphs of Lipschitz-continuous functions of x.

Such "KAM curves" have very strong regularity properties. In particular, for $|\varepsilon|$ small enough, they are analytically conjugated to a rotation by ω; moreover, they are smooth deformations, as ε grows, of the trivial invariant curves $[\Gamma_\omega(0) = \{(x, y) \in \mathscr{C}: y = \omega\}]$ obtained at $\varepsilon = 0$.

On the other hand, if $|\varepsilon|$ is large enough, it can be shown[5] that no such curves exist at all. From now on, by "invariant curve" we shall mean a closed, homotopically nontrivial, invariant curve.

For each $\omega \in (0, 2\pi)$ we can define two "thresholds" in the following way. Let

$$\mathscr{E}(\omega) = \{\varepsilon \geqslant 0 \mid \exists \Gamma_\omega(\varepsilon), \text{ jointly analytic in } \mathbb{T} \times [0, \varepsilon)\}$$

$$\mathscr{E}'(\omega) = \{\varepsilon \geqslant 0 \mid \exists \Gamma_\omega(\varepsilon), \text{ jointly continuous in } \mathbb{T} \times [0, \varepsilon)\}$$

and

$$\varepsilon_c(\omega) = \sup \mathscr{E}_\omega(\varepsilon)$$

$$\varepsilon_c'(\omega) = \sup \mathscr{E}'_\omega(\varepsilon)$$

It is believed that, for the standard map, $\varepsilon_c(\omega) = \varepsilon_c'(\omega)$, but no proof of this exists. The number $\varepsilon_c(\omega)$ is usually called the (*analytic*) *breakdown threshold* for the invariant curve Γ_ω. As a function of ω, $\varepsilon_c(\omega)$ is quite irregular, being in general 0 for each ω rational and nonzero for ω Diophantine.

The breakdown mechanism and, in general, the properties of invariant curves near the critical threshold $\varepsilon_c(\omega)$ are far from being understood.

Here we investigate numerically the regularity properties of the invariant curves and in particular their analytic structure.

First of all, we note that the dynamics may be described in terms of the variable $x \in \mathbb{T}$ only; in fact, $y' = x' - x$ and therefore

$$x_{n+1} - 2x_n + x_{n-1} = \varepsilon f(x_n) \tag{4}$$

where $x_n = F_\varepsilon^n(x_0, y_0)$. Invariant curves may then be found by looking for a change of variables in which the dynamics reduces to a simple rotation by ω:

$$x = \theta + u(\theta) \tag{5}$$

and

$$\theta_n = \theta_{n-1} + \omega = n\omega + \theta_0$$

where of course $1 + u'(\theta) > 0$. It is simple to check that the invariant curve with rotation number ω is given, in parametric form, by

$$x = \theta + u(\theta)$$
$$y = \omega + u(\theta) - u(\theta - \omega)$$

and that the invariant curve shares the same regularity properties of $u(\theta)$, by the implicit function theorem and the above-mentioned theorem of Birkhoff.

The function $u(\theta)$ (from now on called briefly "conjugating function") satisfies the following equation:

$$D_\omega^2 u \equiv u(\theta + \omega) - 2u(\theta) + u(\theta - \omega) = \varepsilon f(\theta + u(\theta)) \tag{6}$$

This equation may be studied perturbatively by expanding $u(\theta)$ in powers of ε and, further, the Taylor coefficients of $u(\theta)$ as Fourier series in θ:

$$u(\theta; \varepsilon) = \sum_{n=1}^{\infty} u_n(\theta)\varepsilon^n = \sum_{n=1}^{\infty} \sum_{k \in \mathbb{Z}} \hat{u}_{n,k} e^{ik\theta} \varepsilon^n \tag{7}$$

Actually, since in our case $f(x)$ is always a trigonometric polynomial containing only sines, $u(\theta)$ is odd and $\hat{u}_{n,k} \in i\mathbb{R}$, $\hat{u}_{n,-k} = -\hat{u}_{n,k}$, as is very easy to check. Moreover, each Taylor coefficient will be a trigonometric polynomial of order increasing with n.

It is natural to study the analytic properties of $u(\theta)$ by investigating the series (7). In particular, we are interested *both* in the analyticity in ε at each fixed θ, *and* the analyticity in θ at fixed ε. In particular, a natural question which arises is to find the relation between the radius of convergence in the complex ε plane of (7) at fixed θ and the KAM breakdown threshold defined above. To be precise, let

$$\rho(\omega) = \inf_{\theta \in \mathbb{T}} (\limsup_{n \to \infty} |u_n(\theta)|^{1/n})^{-1}$$

be the radius of convergence, uniform in θ, of the series (7). Clearly $\rho(\omega) \leqslant \varepsilon_c(\omega)$, since within the radius of convergence of the series (7) there exists

an analytic solution to Eq. (6). It is interesting to study the exact relation between these two "thresholds," as well as to understand the mechanism by which the series (7) ceases to converge as $|\varepsilon|$ grows and therefore $u(\theta; \varepsilon)$ loses analyticity in ε.

A different but related question is the behavior of the same series expansion on the complex θ plane at *fixed* ε *within* the radius of convergence. It is more convenient to pass to complexified dynamical variables as follows:

$$z = e^{ix}$$

$$\zeta = e^{i\theta}$$

$$P(z) = if(x)$$

With these notations, the maps we consider can be written as

$$\frac{z_{n+1} z_{n-1}}{z_n^2} = e^{\varepsilon P(z_n)} \tag{8}$$

where $P(z)$ is a rational function of z with a pole at the origin, such that the coefficients $\{c_n\}$ of its Laurent series at $z = 0$ are real and satisfy $c_{-k} = -c_k$, $c_0 = 0$. In particular. the unit circle in the complex z plane is invariant under this complex dynamics.

Next, let $\phi(\zeta) = e^{i(\theta + u(\theta))}$ and $\gamma = e^{i\omega}$; then ϕ conjugates multiplication by γ (i.e., rotation by ω) on the ζ plane to the dynamics of our complexified map on the z plane. In particular, circles around the origin of radius close enough to 1 on the ζ plane are mapped conformally to analytic, closed invariant curves which wind around the unit circle, as a result of the analytic KAM theory.

The series (7) can be written as a double Taylor–Laurent series:

$$\sum_{n=1}^{\infty} u_n(\theta) \varepsilon^n$$

with

$$u_n(\theta) = \sum_{k \in \mathbb{Z}} \hat{u}_{n,k} \zeta^k$$

and, for each fixed $\varepsilon < \rho(\omega)$, the Laurent series in ζ will converge in an annulus:

$$\sigma^{-1}(\omega, \varepsilon) < |\zeta| < \sigma(\omega, \varepsilon) \tag{9}$$

the two radii being reciprocal for obvious symmetry reasons. We investigate the analytic structure of this series as well, and moreover we study the behavior of $\sigma(\omega, \varepsilon)$ as $\varepsilon \to \rho(\omega)$. Clearly, the annulus in the ζ plane translates to a strip in the complexified θ plane.

2. THE MODELS

We consider maps with

$$f(x) = \sum_{\nu=1}^{\bar{\nu}} \alpha_\nu \sin \nu x \tag{10}$$

where $\alpha_\nu \in \mathbb{R}$, $\bar{\nu} \in \mathbb{N}$, and we will take $\alpha_1 = 1$.

In particular, we analyze in detail the following two- or three-frequency maps:

$$f_1(x) = \sin x + \frac{1}{20} \sin 2x \tag{11}$$

$$f_2(x) = \sin x + \frac{1}{50} \sin 5x \tag{12}$$

$$f_3(x) = \sin x + \frac{1}{30} \sin 3x + \frac{1}{50} \sin 5x \tag{13}$$

$$f_4(x) = \sin x + \frac{1}{20} \sin 2x + \frac{1}{30} \sin 3x \tag{14}$$

Next, we choose a Diophantine (3) rotation number ω. In order to fix the notation, let us introduce the *continued-fraction* expansion. For any irrational number $\omega \in (0, 1)$ let $\{a_k\}_{k \in \mathbb{N}}$ be the sequence of integer numbers such that

$$\frac{\omega}{2\pi} = \cfrac{1}{a_1 + \cfrac{1}{a_2 + \cfrac{1}{a_3 + \ddots}}}$$

Symbolically, we write

$$\frac{\omega}{2\pi} = [a_1, a_2, a_3, \ldots]$$

A trivial computation shows that the continued-fraction expansion of the golden ratio $\omega/2\pi \equiv (\sqrt{5} - 1)/2$ is composed only by one:

$$\frac{\omega_1}{2\pi} = [1, 1, 1, \ldots] = [1^\infty]$$

In analogy to ω_1; we shall consider the numbers

$$\frac{\omega_2}{2\pi} = [2, 2, 2, \ldots] = [2^\infty]$$

and

$$\frac{\omega_3}{2\pi} = [3, 3, 3, \ldots] = [3^\infty]$$

(sometimes referred to as *silver* and *bronze* numbers, respectively). Besides ω_1, ω_2, and ω_3, we consider also *noble* numbers (i.e., those whose continued fraction is definitely one) of the form

$$\frac{\tilde{\omega}_k}{2\pi} = [1, k, 1, 1, \ldots] = [1, k, 1^\infty]$$

3. RESULTS

For all the maps considered we found natural boundaries in the complex ε plane, as was found for the standard map in ref. 2. The natural boundaries appear to be closed curves, symmetric with respect to the real axis [since the coefficients of the Taylor series in (7) are real], but not circles.

A simple symmetry argument shows that when the Fourier expansion of $f(x)$ contains only odd frequencies, then the natural boundary must be

Table I. Radius of Convergence and Breakdown Threshold[a]

	$\bar{\rho}$	$\bar{\varepsilon}_c$	$\bar{\bar{\varepsilon}}_c$
$f_1(x), \omega_1$	0.8	1.2	1.2
$f_2(x), \omega_3$	0.6	0.7	0.67
$f_3(x), \omega_1$	0.5	0.5	0.5
$f_4(x), \omega_1$	0.7	0.9	0.9
$f_1(x), \tilde{\omega}_1$	0.75	1.1	1.13
$f_2(x), \tilde{\omega}_1$	0.45	0.6	0.64

[a] Here $\bar{\rho}$ is an estimate of the radius of convergence of the series (7) based on Padé approximants; $\bar{\varepsilon}_c$ is an estimate of the breakdown threshold based on Padé approximants; $\bar{\bar{\varepsilon}}_c$ is an estimate of the breakdown threshold based on Greene's method. The maps $f_1, \ldots, f_4$ are defined in Eqs. (11)–(14) and the notation for the rotation numbers is the same as in Section 2.

symmetric with respect to the imaginary ε axis (cf. Figs. 2 and 3): in fact, if $f(x)$ contains only odd frequencies, $P(z)$ is an odd function and (8) is invariant under the transformation $z \mapsto -z$, $\varepsilon \mapsto -\varepsilon$. This symmetry property implies the observed symmetry in the distribution of the singularities of u.

The intersection of the natural boundary with the positive real axis in the complex ε plane coincides with the threshold found by Greene's method, within numerical errors (see Table I; a review of Greene's method is presented in Appendix A). It is interesting to note that, since for some maps the natural boundary appears to elongate in the direction of the real axis (see Table I and Fig. 2, which shows the natural boundary for, e.g., the invariant curve with rotation number ω_3 of the map with nonlinear term f_2), it follows that for those maps the radius of convergence $\rho(\omega)$ of the series (7) is *strictly less than* the breakdown threshold $\varepsilon_c(\omega)$.

We note also that for all the maps of the type we considered (including those for which we do not show the singularities of Padé approximants, for

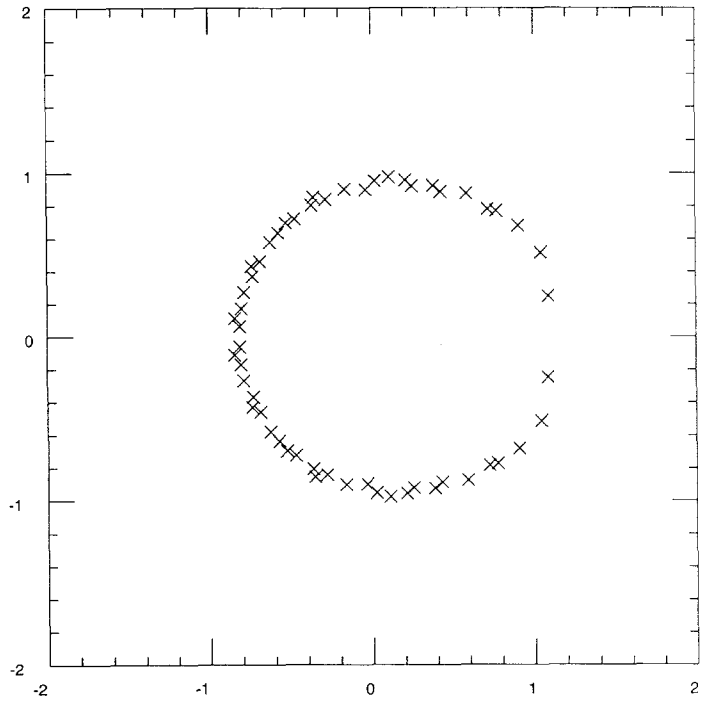

Fig. 1. Poles of the Padé approximants [70/70] in ε for the map with $f(x) = \sin x + 1/20 \sin 2x$, rotation number ω_1, $\theta = 1$.

brevity), for all Diophantine rotation numbers of the above-mentioned type, a natural boundary in the complex ε plane was found. Some natural questions therefore arise: are there maps with a sufficiently regular nonlinear term f such that a different behavior occurs? How "universal" are natural boundaries in perturbation expansions for invariant tori of Hamiltonian systems? What is the relation between the shape of the natural boundaries, the frequencies in the Fourier expansion of f, and the continued-fraction expansion of ω? If, indeed, we face a universal feature—at least within the class of maps considered—it should be possible to understand it in a "renormalization group" framework of the type devised in ref. 6.

In the complex ζ plane, all the maps we considered have natural boundaries on the annulus of convergence of the Laurent series (9). A similar natural boundary was found, with very different techniques, by Greene and Percival[7] for the standard map and for the semistandard map. We show the same boundary directly by showing the singularities of Padé

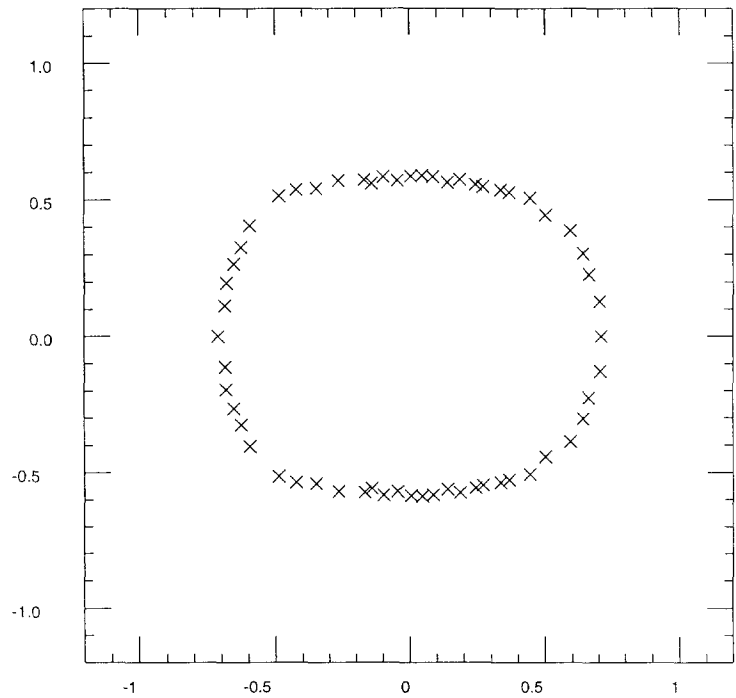

Fig. 2. Poles of the Padé approximant [70/70] in ε for the map with $f(x) = \sin x + 1/50 \sin 5x$, rotation number ω_3, $\theta = 1$.

approximants of higher order in the complex ζ plane. Moreover, the same phenomena occur for all the other maps considered, remarkably always with boundaries of annular shape—quite differently than the case of boundaries on the complex ε plane, where the shape depends on f and on ω.

We also measured the external radius of the annululs $\sigma(\omega, \varepsilon)$ and determined numerically its dependence on ε. In the case of the semi-standard map [i.e., the case $f(x) = e^{ix}$], since the order n in ε of the expansion (7) contains only the frequency $k = n$, the expansion can be considered one in the variable $\varepsilon e^{i\theta} = \varepsilon\zeta$; it follows that $\sigma(\omega, \varepsilon)$ tends to 0 linearly as ε tends to the radius of convergence of the series. In the case of the standard map and of the other, more complex maps considered in this paper, this argument of course does not work, but it is remarkable to note that the width of the analyticity region in the ζ plane still appears to tend linearly to 0 [and $\sigma(\omega, \varepsilon)$ to 1] as $\varepsilon \to \varepsilon_c(\omega)$.

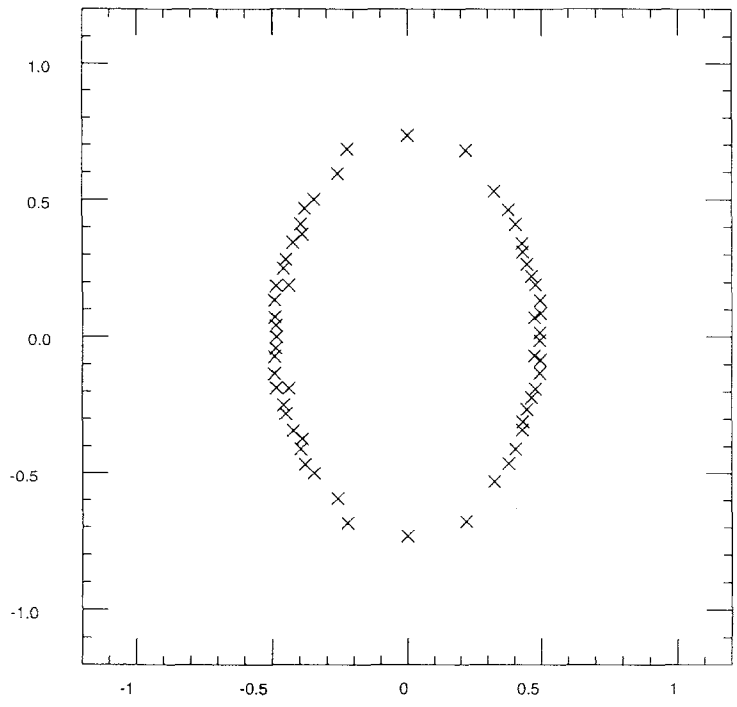

Fig. 3. Poles of the Padé approximant [70/70] in ε for the map with $f(x) = \sin x + 1/30 \sin 3x + 1/50 \sin 5x$, rotation number ω_1, $\theta = 1$.

Again, this phenomenology seems to be "universal" among the maps considered here. It is rather easy, though, to write a counterexample in which *no* natural boundary appears for a given invariant curve at a given ε; in particular, we can exhibit a map of the type (1), (2) which has an invariant curve, say with rotation number equal to the golden mean, such that its conjugating function is an *entire* function of θ for, e.g., $\varepsilon = 1/2$. In fact, let

$$u_{\omega_1}(\theta, \tfrac{1}{2}) = \tfrac{1}{2} \sin \theta$$

and let $w(x)$ be the inverse function of $\theta + 1/2 \sin \theta$; then, since for all ω Diophantine, ε, and θ Eq. (6) must be satisfied, a simple calculation shows that if we take

$$f(x) = 2[\cos \pi(\sqrt{5} - 1) - 1] \sin w(x)$$

then (6) will have $1/2 \sin \theta$ as solution for $\omega = \omega_1$ and $\varepsilon = 1/2$.

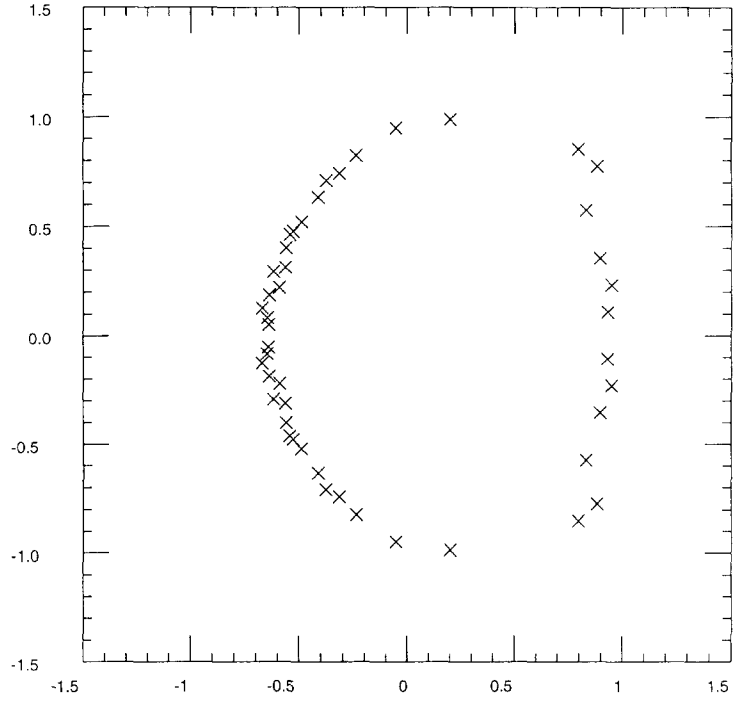

Fig. 4. Poles of the Padé approximant [70/70] in ε for the map with $f(x) = \sin x + 1/20 \sin 2x + 1/30 \sin 3x$, rotation number ω_1, $\theta = 1$.

Besides the examples considered in this paper, we studied a large variety of mappings of the type given by Eqs. (1), (2), and (10) with rotation numbers of the type mentioned in Section 2. The results (not presented here, for brevity) show a phenomenology similar to the cases studied here. We just mention some of them in Table I, where the radius of convergence and the breakdown threshold as determined by the Padé approximant method and the breakdown threshold as determined with Greene's method are reported.

We give selected figures showing the shapes of the natural boundary in the complex ε plane (Figs. 1–4) and in the complex ζ plane (Figs. 5–7).

Finally, in Figs. 8 and 9 we show how $\sigma(\omega, \varepsilon)$ tends to 1 *linearly* as $\varepsilon \to \rho(\omega)$.

APPENDIX A. GREEN'S METHOD

The most reliable numerical method to determine the breakdown of invariant curves is the one developed by Greene.[8] The results provided by

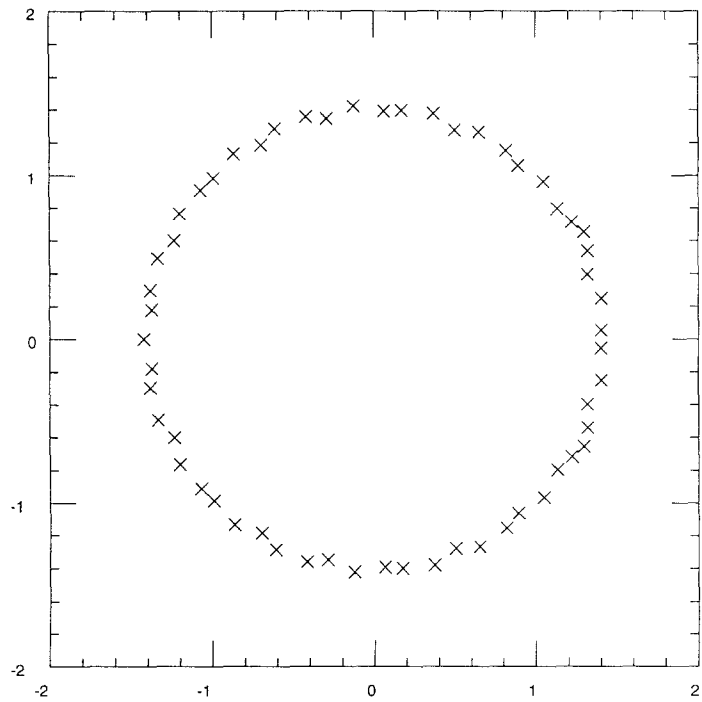

Fig. 5. Poles of the Padé approximant [80/80] in ζ for the standard map, $\varepsilon = 0.7$.

this method will form the basis of comparison and interpretation of ours. In this perspective we consider it worthwhile to dedicate a few words to a review of the method.

Greene's starting point is the conjecture that the breakdown of an invariant curve is related to a transition from stability to instability of the periodic orbits approaching the invariant curve. More precisely, for any irrational ω, let $\{p_k/q_k\}_{k\in\mathbb{Z}}$ be the sequence of rational approximants to ω such that $p_k/q_k \to \omega$ as $k \to \infty$. Let us denote by $\mathscr{P}(p_k/q_k)$ a periodic orbit with frequency p_k/q_k. The critical breakdown threshold is found as the value of ε at which the periodic orbits $\mathscr{P}(p_k/q_k)$ are *alternatively* stable or unstable. To determine the stability of $\mathscr{P}(p_k/q_k)$, we compute the Floquet multipliers of the linearized map. In particular, the tangent space orbit $(\delta y_n, \delta x_n)$ at the point (y_n, x_n) is defined in terms of the initial conditions $(\delta y_0, \delta x_0)$ through a matrix A as

$$\begin{bmatrix} \delta y_n \\ \delta x_n \end{bmatrix} = A \begin{bmatrix} \delta y_0 \\ \delta x_0 \end{bmatrix}$$

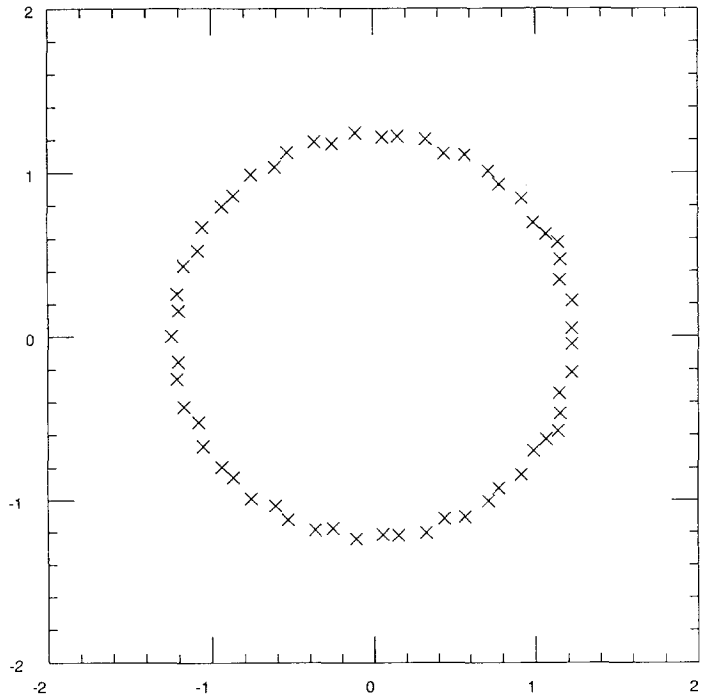

Fig. 6. Poles of the Padé approximant [80/80] in ζ for the standard map, $\varepsilon = 0.8$.

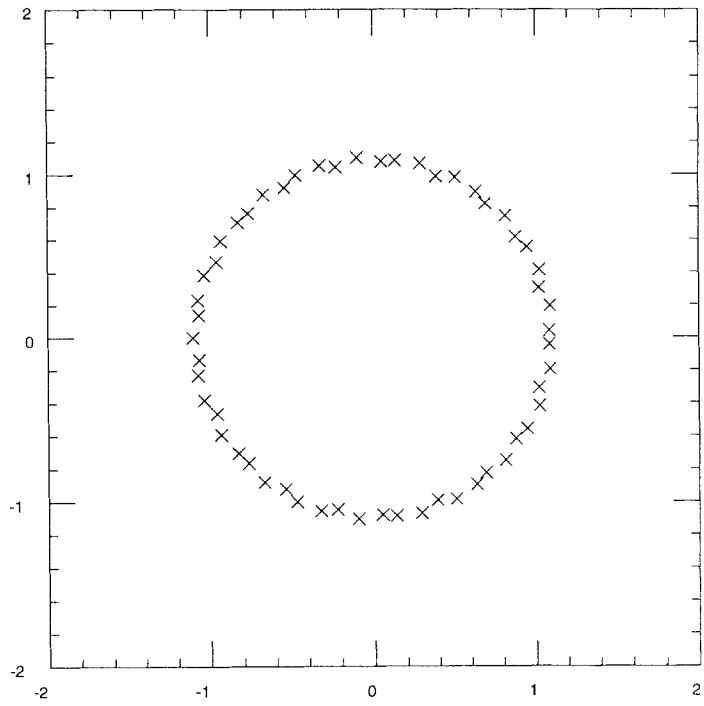

Fig. 7. Poles of the Padé approximant [80/80] in ζ for the standard map, $\varepsilon = 0.9$.

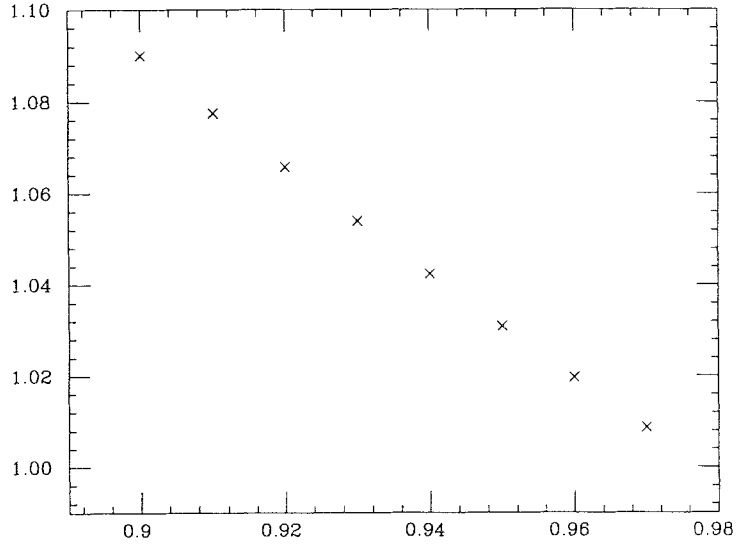

Fig. 8. $\sigma(\omega, \varepsilon)$ vs. ε for the standard map, rotation number ω_1.

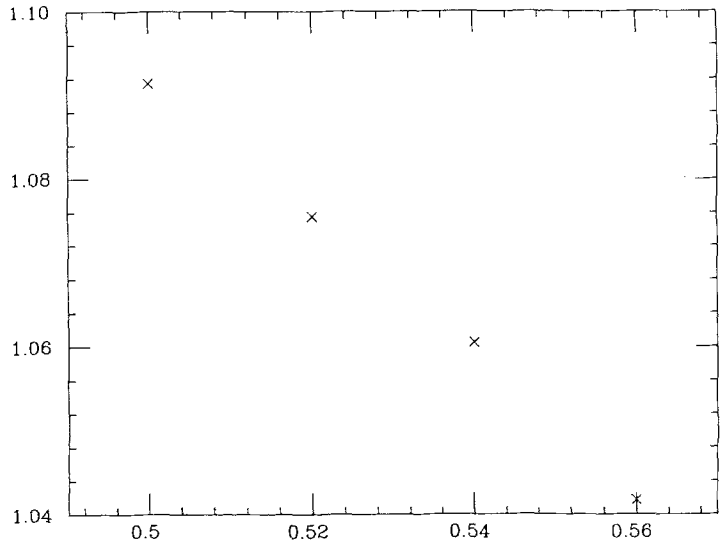

Fig. 9. $\sigma(\omega, \varepsilon)$ vs. ε for the map with $f(x) = \sin x + 1/50 \sin 5x$, rotation number ω_1.

where, in our case, the matrix A associated to the periodic orbit $\mathscr{P}(p_k/q_k)$ is given by

$$A = \prod_{i=1}^{q_k} \begin{bmatrix} 1 - \varepsilon \sum_{\nu=1}^{\bar{\nu}} \alpha_\nu \nu \cos \nu x_i & 1 \\ -\varepsilon \sum_{\nu=1}^{\bar{\nu}} \alpha_\nu \nu \cos \nu x_i & 1 \end{bmatrix}$$

The Floquet multipliers of the linearization are the eigenvalues $\lambda_{1,2}$ of the matrix A. Since the map is area-preserving, such eigenvalues depend only on the trace of A. More precisely, if we set

$$R = \tfrac{1}{4}[2 - \mathrm{Trace}(A)]$$

(called by Greene the *residue* of the periodic orbit), the eigenvalues $\lambda_{1,2}$ of A are given by the expression

$$\lambda_{1,2} = 1 - 2R \pm 2[R(R-1)]^{1/2}$$

When $0 < R < 1$ the periodic orbit is stable, since the eigenvalues are complex with modulus 1. On the other hand, the orbit is unstable when $R < 0$ or $R > 1$.

Therefore once a periodic orbit is found, the calculation of the residue R determines its stability. The breakdown threshold of an invariant curve

(with rotation number ω) is then defined as the value of ε at which the periodic orbits $\mathscr{P}(p_k/q_k)$ (with frequencies equal to the rational approximants to ω) are alternatively stable and unstable.

Numerically, the most delicate point is certainly the determination of the periodic orbits. By definition of a periodic orbit, to find $\mathscr{P}(p_k/q_k)$, one has to find a point (x_0, y_0) which is equal to the q_kth iterate of the mapping $(x_0 = x_{q_k}, y_0 = y_{q_k})$, with the further constraint that $\sum_{i=1}^{q_k} y_i = p_k$. Here (x_{q_k}, y_{q_k}) are obtained by the recursive relations

$$y_{n+1} = y_n + \varepsilon \sum_{\nu=1}^{\bar{\nu}} \alpha_\nu \sin \nu x_n$$

$$x_{n+1} = x_n + y_{n+1}$$

Notice that since (by definition) $q_k \to \infty$ as $k \to \infty$, the determination of $\mathscr{P}(p_k/q_k)$ may require a substantial amount of CPU time for large k.

To ease this problem, Greene observed (see Appendix A of ref. 8), using the symmetry of the map, that the initial point of the periodic orbit belongs to the lines $x_0 = y_0/2$, $y_0/2 + \pi$, or $x_0 = 0$, π. In fact, the map can be written as a product of two involutions:

$$F_\varepsilon = I_1 I_2$$

with $I_1^2 = I_2^2 = 1$; it is then possible to show[8] that if (x_0, y_0) is a fixed point of I_1 (or I_2) and $F_\varepsilon^N(x_0, y_0)$ is also a fixed point for some $N \in \mathbb{N}$, then the orbit with initial point (x_0, y_0) is periodic with period $2N$.

A simple calculation shows that I_1 and I_2 are given by

$$I_1: \begin{cases} x_n = -x_{n-1} \\ y_n = y_{n-1} + \varepsilon \sum_{\nu=1}^{\bar{\nu}} \alpha_\nu \sin \nu x_n \end{cases}$$

and

$$I_2: \begin{cases} x_{n+1} = -x_n + y_n \\ y_n = y_n \end{cases}$$

The fixed points of I_1 are at $x = 0$ and $x = \pi$, while those of I_2 are at $x = y/2$ or $x = y/2 + \pi$.

APPENDIX B. CALCULATION OF PADÉ APPROXIMANTS

Given a formal Taylor series

$$\sum_{n=0}^{\infty} a_n z^n \tag{B1}$$

its Padé approximants are the rational approximants, traditionally denoted by $[M, N]$, defined in the following way:

$$[M, N] \equiv \frac{P_M(z)}{Q_N(z)}$$

where $P_M(z)$, $Q_N(z)$ are polynomials of degree M, N, respectively, such that the Taylor expansion of their quotient agrees up to order $M+N$ with the series (B1). $Q_N(z)$ is usually normalized by the condition $Q_N(0)=1$. In the Padé approximants $[M/N]$ there are therefore $M+N+1$ indeterminate coefficients as in any polynomial of degree $M+N$. These coefficients can be formally determined from first $M+N+1$ terms of (B1). To minimize roundoff errors, the Padé approximants are computed recursively with the following formulas:

$$P_{2j}(x)/Q_{2j}(x) = [N-j/j]$$
$$P_{2j+1}(x)/Q_{2j+1}(x) = [N-j-1/j]$$

and

$$\frac{P_{2j}(x)}{Q_{2j}(x)} = \frac{(\bar{P}_{2j-1}P_{2j-2}(x) - x\bar{P}_{2j-2}P_{2j-1}(x))/\bar{P}_{2j-1}}{(\bar{P}_{2j-1}Q_{2j-2}(x) - x\bar{P}_{2j-2}Q_{2j-1}(x))/\bar{P}_{2j-1}}$$
$$\frac{P_{2j+1}(x)}{Q_{2j+1}(x)} = \frac{(\bar{P}_{2j}P_{2j-1}(x) - \bar{P}_{2j-1}P_{2j}(x))/(\bar{P}_{2j} - \bar{P}_{2j-1})}{(\bar{P}_{2j}Q_{2j-1}(x) - \bar{P}_{2j-1}Q_{2j}(x))/(\bar{P}_{2j} - \bar{P}_{2j-1})}$$

where $\bar{P}_j$ is the coefficient of the highest power in $P_j(x)$, and the recursion is initialized by setting $P_0(x)$ and $P_1(x)$ to the N and $N-1$ Taylor polynomials respectively:

$$P_0(x) = \sum_{k=0}^{N} a_k x^k, \qquad Q_0(x) = 1$$
$$P_1(x) = \sum_{k=0}^{N-1} a_k x^k, \qquad Q_1(x) = 1$$

For a complete reference see ref. 9.

To identify a natural boundary, we compute "diagonal" Padé approximants $[N/N]$ (considered to be the most accurate) for increasing N and look at how the poles of the approximants behave: in the presence of a natural boundary, they will cluster on the boundary curve as N grows. For a reliable identification it is necessary in our case to compute Padé approximants up to high orders, say [70/70] or [80/80].

It is common to have, besides "genuine" poles and zeros, also fake pole–zero pairs which cancel (a so-called "ghost"). It is possible to distinguish them from a genuine pole and a genuine zero nearby (a situation very frequent when dealing with natural boundaries, essential singularities, and accumulation points of singularities) because ghosts disappear as any parameter in the series is slightly varied, or the order of the approximants changes. Moreover, the distance between the pole and the zero in a ghost is always close to machine precision, and in any case several orders of magnitude smaller than the distance in a genuine pole–zero pair. A semiautomatic filtering mechanism can therefore be used. Finally, we remark that since the series we consider have an almost lacunar nature, as N increases, ghosts tend to appear and disappear with a certain regularity as peaks are crossed.

APPENDIX C. CALCULATION OF THE PERTURBATION EXPANSION

The coefficients of the perturbative expansion (7) are computed with the following formulas, valid when $f(x)$ is given by (10):

$$b_0^{(\nu)}(\theta) = e^{i\nu\theta} \qquad \text{for} \quad \nu = 1,\ldots,\bar{\nu}$$

$$u_n(\theta) = D_\omega^{-2} \operatorname{Im}\left(\sum_{\nu=1}^{\bar{\nu}} \alpha_\nu b_{n-1}^{(\nu)} \right) \qquad \text{for} \quad n \geqslant 1$$

$$b_n^{(\nu)}(\theta) = \frac{i\nu}{n} \sum_{l=1}^{n} l u_l(\theta)\, b_{n-l}^{(\nu)}(\theta) \qquad \text{for} \quad n \geqslant 1$$

Next we expand in Fourier series u and the b's; first we note that since $u(\theta)$ is real and odd in θ, $\hat{u}_k$ is purely imaginary and odd in k, so we set $\hat{v}_{n,k} = i\hat{u}_{n,k}$, with $\hat{v}_{n,k} \in \mathbb{R}$. We obtain

$$\hat{b}_{0,k}^{(\nu)} = \delta_{\nu,k} \tag{C1}$$

$$\hat{v}_{n,k}^{\nu} = \frac{1}{2D_{\omega,k}^2} \sum_{\nu=1}^{\bar{\nu}} \alpha_\nu (\hat{b}_{n-1,k}^{(\nu)} - \hat{b}_{n-1,-k}^{(\nu)}) \tag{C2}$$

$$\hat{b}_{n,k}^{(\nu)} = \frac{\nu}{n} \sum_{l=1}^{n} \sum_{h=h_{\min}}^{h_{\max}} \hat{v}_{l,h} \hat{b}_{n-l,k-h}^{(\nu)} \tag{C3}$$

with $n \geqslant 1$; in (C2), $1 \leqslant k \leqslant \bar{\nu}n$, while in (C1) and (C3), $-\bar{\nu}n \leqslant k \leqslant \nu n$; moreover, $h_{\min} = -\min(l, (n-l)-k)$, $h_{\max} = \min(l, (n-l)+k)$, and $\hat{D}_{\omega,k}^2 = 2(\cos k\omega - 1)$.

ACKNOWLEDGMENTS

All computations have been performed on several VAX/VMS computer systems at the Dipartimento di Matematica, II Università di Roma (Tor Vergata), Facoltà di Scienze, Università dell'Aquila, and Institute of Scientific Interchange, Torino. We are grateful to R. De La Llave and G. Gallavotti for very helpful suggestions and encouragement. A. B. and A. C. wish to express gratitude to Profs. M. Rasetti, R. Livi, and S. Ruffo for their invitations at the workshops "Complexity and Evolution" at the Institute of Scientific Interchange, Torino, where part of this work was done, and for many helpful discussions.

REFERENCES

1. A. Celletti and L. Chierchia, Construction of analytic KAM surfaces and effective stability bounds, *Commun. Math. Phys.* **118**:119 (1988).
2. A. Berretti and L. Chierchia, On the complex analytic structure of the golden invariant curve for the standard map, *Nonlinearity* **3**:39–44 (1990).
3. R. S. MacKay, Transition to chaos for area-preserving maps, in *Lecture Notes in Physics*, Vol. 247 (Springer-Verlag, Berlin, 1985), p. 390.
4. J. Moser, Recent developments in the theory of Hamiltonian systems, *SIAM Rev.* **28**:459 (1986).
5. J. N. Mather, *Ergodic Theory Dynam. Syst.* **4**:301 (1984); R. S. MacKay and I. C. Percival, Converse KAM: Theory and practice, *Commun. Math. Phys.* **98**:469 (1985).
6. D. F. Escande and F. Doveil, Renormalization method for computing the threshold of large-scale stochastic instability in two degrees of freedom Hamiltonian systems, *J. Stat. Phys.* **26**:257 (1981).
7. J. M. Greene and I. C. Percival, Hamiltonian maps in the complex plane, *Physica* **3D**:530 (1981).
8. J. M. Greene, A method for determining a stochastic transition, *J. Math. Phys.* **20**:1183 (1979).
9. G. Baker, *Essentials of Padé Approximants* (Academic Press, New York, 1975).